

Supplemental Methods:

Plasmids – mHIF-1 α (747-836) was amplified by PCR and cloned into pET32a (Novagen) to generate pET32a mHIF-1 α (747-836). pET32a hHIF-1 α (737-826) and pGal hHIF-1 α (737-826) have been described previously (1), and were used as templates for site-directed mutagenesis (Quikchange, Stratagene) to generate hHIF-1 α N803A, RLL781-783 AAA, R781A and LL782-783AA mutants. hHIF-1 α (737-826) wildtype and RLL781-783 AAA inserts were digested from pET32a and cloned into pEGST (2), to generate an N-terminal GST fusion. pRL-TK was obtained from Promega, and pG5E1B-Luc (Gal-4 reporter plasmid) has been described previously (3). Full-length mFIH was amplified by PCR and cloned into pMBP to give an N-terminal MBP tag. pMBP hFIH, pET32a-TEV hFIH and pET32a mNotch1 RAM (1753-1847) have been described previously (4). pET32a mNotch1 ARD (1862-2104) and pET32a mNotch4 ARD (1570-1815) have also been described previously (5) and were used as templates for site-directed mutagenesis (Quikchange, Stratagene) to generate the Notch1 mutants N1945Q, N2012Q, N1945Q/N2012Q, A1944P/N2012Q, I1946Q/N2012Q, and the Notch4 mutants P1655I and Q1657I. The chimeric construct pET32a Notch-HIF linker was generated by overlap extension PCR, in which one of the β -hairpin regions (residues 1940-1953) in the N2012Q mutant of the mNotch1 ARD was replaced with a linker consisting of mHIF-1 α residues 808-825. pET32a HIF-Notch helix was generated by PCR and consisted of mHIF-1 α (747-836) with the last 18 amino acids (819-836) replaced by helix-3A from mNotch1 (residues 1950-1963). Full-length hGankyrin was amplified by PCR and cloned into pET32a. An N-terminal GST tag was amplified from pGEX-4T-1 (GE Healthcare) and inserted into pET32 at the EcoRI site upstream of the Gankyrin ORF. The C-terminal domain of hS6-ATPase (S6-C, residues 337-418) was amplified by PCR using a reverse primer (5'-CATGAATTCTGTTTCCTCAACACTTGTA AAAACTCATGCTCCTG-3') that included an internal ribosome entry site downstream of the S6-C stop codon. This was inserted into the pET32a Gankyrin construct to create a di-cistronic transcript, in which Trx-6H-S6-C and Gankyrin are separately translated from a single transcript. pAC28-H6-TEV was generated by insertion of a 6-histidine-TEV oligonucleotide linker (Upper 5'-CATGGGTGGCTCCCATCACCATCACCATCACGACTACGATATCCCGACCACCGAAAACCTGTACTTCCAGGGCGC-3', Lower, 5'-CATGGCGCCCTGGAAGTACAGGTTTTTCGGTGGTCCGGATATCGTAGTCGTGATGGTGTGTTGGTATGGGAGCCACC-3') into the NcoI site of the pAC28 plasmid (2). The upstream NcoI site was subsequently mutated, and an oligonucleotide containing a multiple cloning site based on that of pET32a was then inserted between the NcoI and HindIII sites (Upper, 5'-CATGGCTGGTACCGATATCGGATCCGAATTCGAGCTCCGTCGACA-3', Lower, 5'-AGCTTGTCGACGGAGCTCGAATTCGGATCCGATATCGGTACCAGC-3'). The resultant vector encodes an N-terminal H6-tag that can be cleaved by TEV protease. To generate proteins with minimal tags for structural analysis, mHIF-1 α (747-836), Notch-HIF linker, hGankyrin, mFIH, mNotch1 ARD wildtype and N2012Q fragments were excised from pET32 and cloned into pAC28-H6-TEV. All constructs were verified by sequencing.

Supplemental Figure S1. Gankyrin is hydroxylated on a single Asn residue within the ARD.

Trx-6H-tagged wildtype and Asn-Ala mutants of full-length human Gankyrin (65 μ M) were analysed for hydroxylation by MBP-hFIH (2.5 μ M), as inferred by 2OG turnover in CO₂ capture assays. The RAM domain of Notch, which is not hydroxylated by FIH (5), was included as a negative control. Data are the mean of triplicate reactions \pm SD and are representative of >3 independent experiments. These data support the previously reported hydroxylation of Asn100 in Gankyrin (6), and indicate that it is likely to be the predominant site of hydroxylation by FIH.

Supplemental Figure S2. Notch Peptides are disordered in solution.

A, Sequence alignment of Long (35-mer) and Short (20-mer) mNotch1 Site 1 peptides described in (7). The Asn residue hydroxylated by FIH, Asn1945, is indicated (#). Elements of secondary structure adopted by these residues within the context of the full-length ARD are shown above the sequence. B, Far-UV CD analyses of the peptides from (A) indicate that they are both disordered in solution.

Proteins were analysed at concentrations of 0.2 mg/ml in 5 mM sodium phosphate, pH 8.0. Data were converted to mean residue ellipticity and normalised to the ellipticity at 207 nm (8), and are the average of three independent scans.

Supplemental Figure S3. Conservative mutation of the target Asn residues in the mNotch1 ARD prevents hydroxylation by FIH.

A, Site-directed mutagenesis was performed to replace the Asn residues at Site 1 (N1945) and Site 2 (N2012) with Gln residues. Trx-6H-tagged wildtype and mutant mNotch1 ARD proteins (50 μ M) were tested as substrates in CO₂ capture assays with recombinant MBP-mFIH (0.5 μ M), which inferred that Gln-mutation of these residues abolishes hydroxylation by FIH. B, Far-UV CD spectroscopy was employed to analyse the structures of the Notch1 wildtype and N2012Q mutant (Notch1^{S2*}) ARD proteins. Proteins were analysed at concentrations of 0.2 mg/ml in 5 mM sodium phosphate, pH 8.0. Data were converted to mean residue ellipticity and normalised to the ellipticity at 207 nm, and are the average of three independent scans. The CD profiles for the two proteins were very similar, indicating that the structure of the Notch1 ARD is not significantly influenced by mutation of the Site 2 Asn to Gln. C, Far-UV CD spectra are shown for Trx-6H-tagged mNotch1^{S2*} (N2012Q), Notch1^{S2*} A-P (A1944P/N2012Q), Notch1^{S2*} I-Q (I1946Q/N2012Q), Notch4 P-A (P1655A) and Notch4 Q-I (Q1657I) ARD proteins. The concentration of each protein was 0.2 mg/ml in 5 mM sodium phosphate, pH 8.0. Data were converted to mean residue ellipticity and normalised to the ellipticity at 207 nm (8), and are representative of three independent scans.

Supplemental Figure S4. Detailed depiction of Notch peptide conformations. The hydroxylated Asn residue and Fe²⁺ ion (tan) are centred in each field of view. All atoms of Notch peptides are shown, while FIH is shown in cartoon format (grey). *A* A water-bridged hydrogen bond between the backbone N-H in the -1 and +1 position maintains the turn conformation around Asn 1945. *B*, *C* A Pro residue (mNotch-1 A1944P and wt mNotch-4, respectively) in the -1 position prevents this hydrogen bonding pattern, and the peptide adopts a more extended conformation. *D* mNotch-4 Q1657I: the unrestrained peptide forms a hydrophobic interaction between Pro and Ile residues at -1 and +1, compensating for the lack of hydrogen bonding.

Supplemental Table S1. Estimation of secondary structure from CD spectra.

Raw data (baseline corrected) from far-UV CD spectroscopy collected in the 190-260 nm range were analysed using the DICHROWEB server (9), and the CDSSTR deconvolution method (10) was used to estimate the secondary structural content using reference set 7. The estimated content of both regular (r) and disordered (d) helix and strand are shown. Data are the average of three experiments (from at least 2 independent protein preparations) \pm SD.

Supplemental References

1. Linke, S., Stojkoski, C., Kewley, R. J., Booker, G. W., Whitelaw, M. L., and Peet, D. J. (2004) *J Biol Chem* **279**, 14391-14397
2. Kholod, N., and Mustelin, T. (2001) *Biotechniques* **31**, 322-323, 326-328
3. Novitch, B. G., Spicer, D. B., Kim, P. S., Cheung, W. L., and Lassar, A. B. (1999) *Curr Biol* **9**, 449-459
4. Linke, S., Hampton-Smith, R. J., and Peet, D. J. (2007) *Methods Enzymol* **435**, 61-85
5. Zheng, X., Linke, S., Dias, J. M., Gradin, K., Wallis, T. P., Hamilton, B. R., Gustafsson, M., Ruas, J. L., Wilkins, S., Bilton, R. L., Brismar, K., Whitelaw, M. L., Pereira, T., Gorman, J. J., Ericson, J., Peet, D. J., Lendahl, U., and Poellinger, L. (2008) *Proc Natl Acad Sci U S A* **105**, 3368-3373
6. Cockman, M. E., Lancaster, D. E., Stolze, I. P., Hewitson, K. S., McDonough, M. A., Coleman, M. L., Coles, C. H., Yu, X., Hay, R. T., Ley, S. C., Pugh, C. W., Oldham, N. J., Masson, N., Schofield, C. J., and Ratcliffe, P. J. (2006) *Proc Natl Acad Sci U S A* **103**, 14767-14772
7. Wilkins, S. E., Hyvarinen, J., Chicher, J., Gorman, J. J., Peet, D. J., Bilton, R. L., and Koivunen, P. (2009) *Int J Biochem Cell Biol* **41**, 1563-1571

8. Raussens, V., Ruysschaert, J. M., and Goormaghtigh, E. (2003) *Anal Biochem* **319**, 114-121
9. Whitmore, L., and Wallace, B. A. (2004) *Nucleic Acids Res* **32**, W668-673
10. Johnson, W. C. (1999) *Proteins* **35**, 307-312

Figure S1

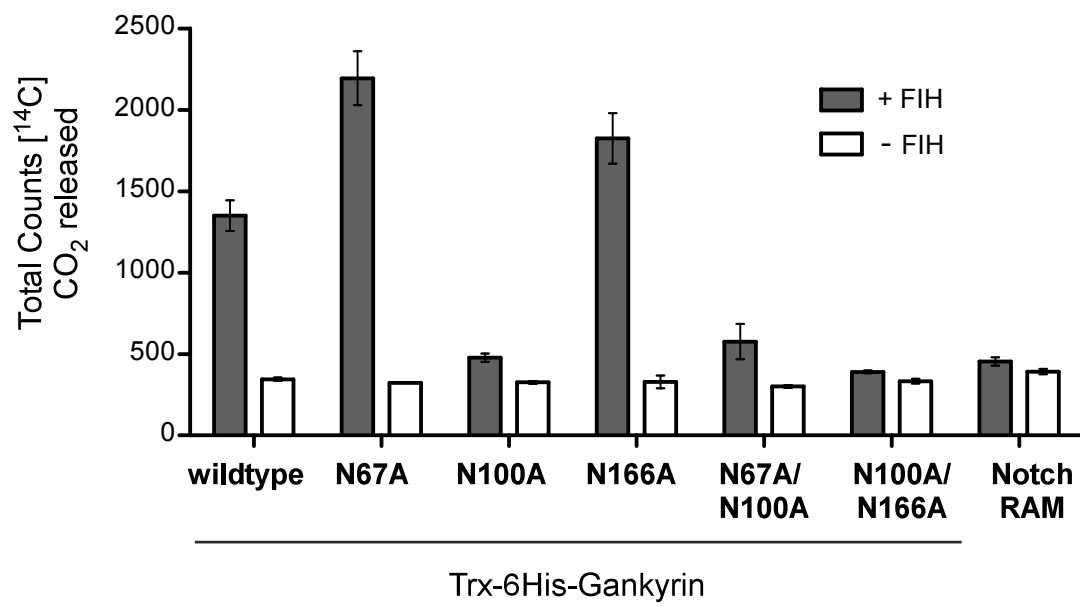


Figure S2

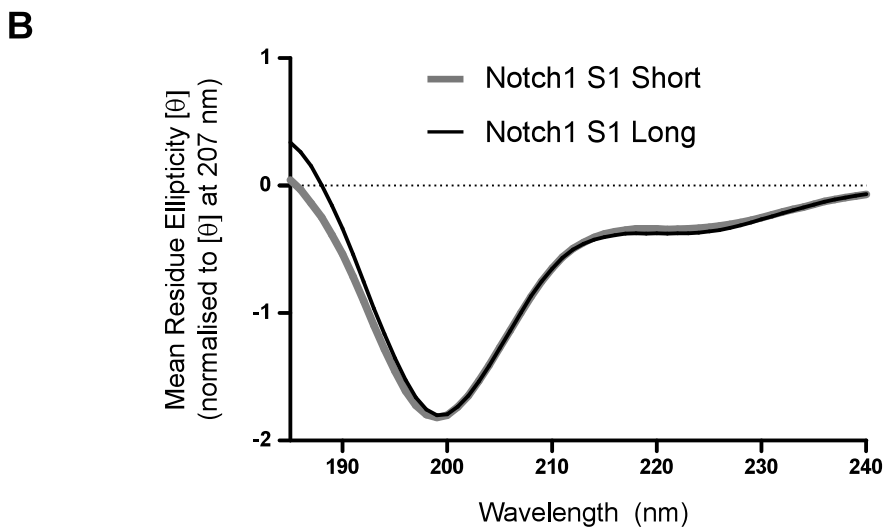
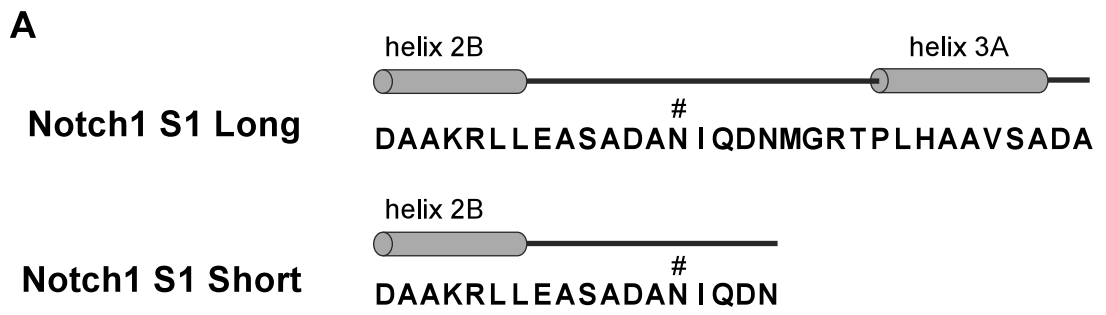


Figure S3

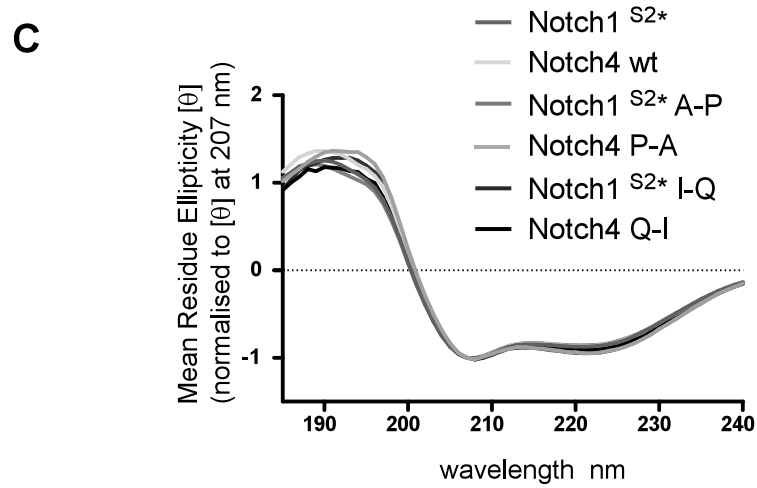
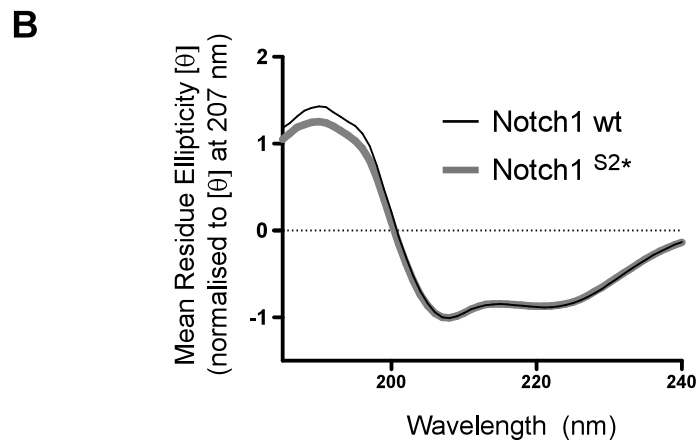
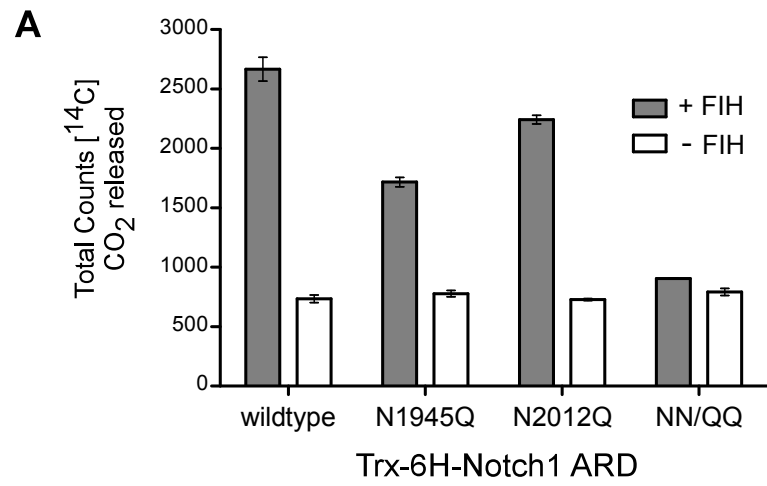


Figure S4

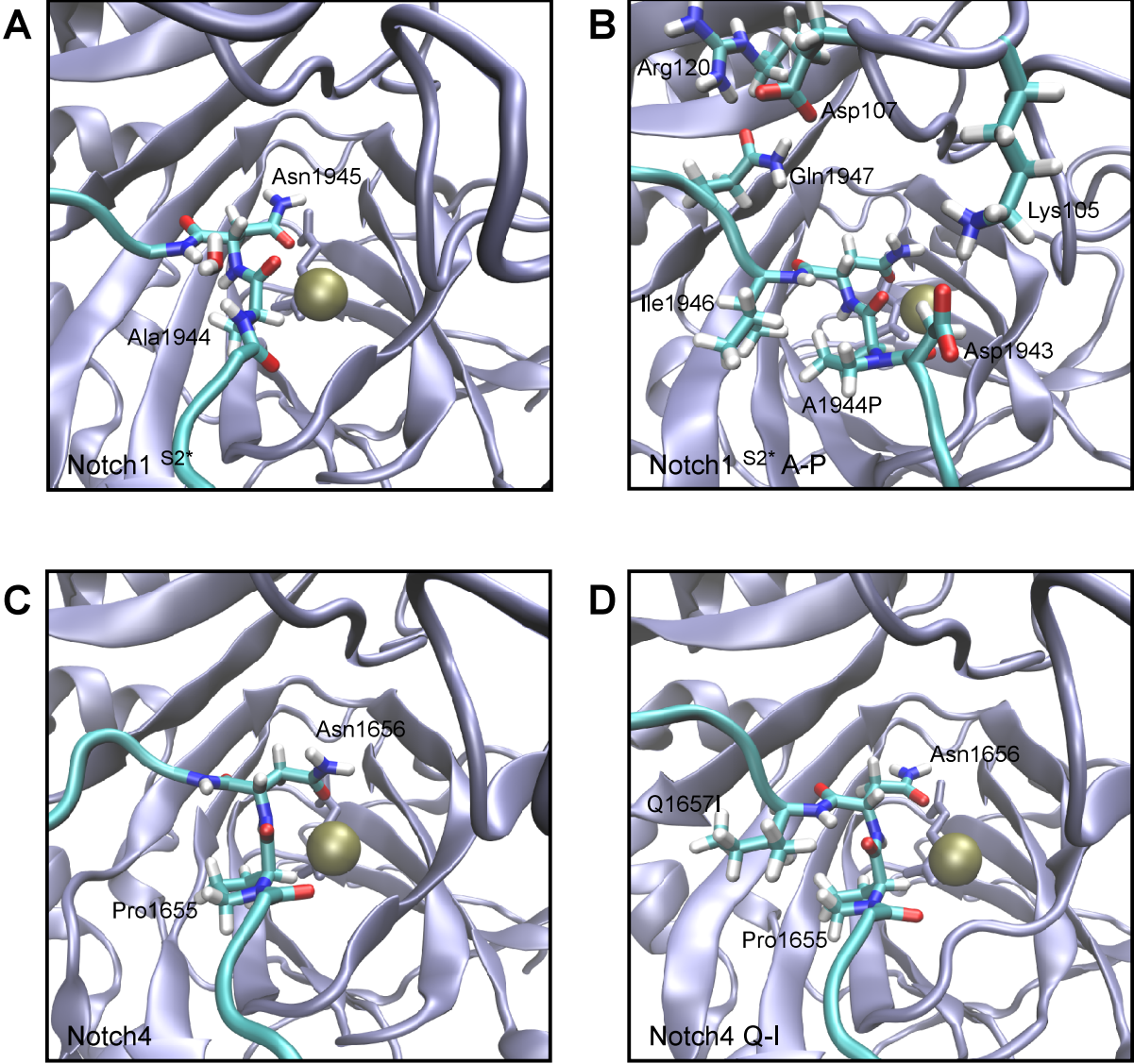


Table S1

6H-mFIH	0.12 ± 0.01	0.10 ± 0.00	0.14 ± 0.01	0.09 ± 0.00	0.19 ± 0.00	0.35 ± 0.01	0.99 ± 0.01
6H-mNotch1 ARD	0.10 ± 0.01	0.10 ± 0.00	0.16 ± 0.01	0.08 ± 0.01	0.18 ± 0.01	0.36 ± 0.02	0.99 ± 0.01
6H-hGankyrin	0.24 ± 0.01	0.17 ± 0.01	0.09 ± 0.01	0.07 ± 0.00	0.19 ± 0.01	0.23 ± 0.01	0.99 ± 0.01
6H-Notch1 S2*	0.11 ± 0.01	0.09 ± 0.01	0.13 ± 0.01	0.08 ± 0.00	0.16 ± 0.01	0.41 ± 0.01	0.98 ± 0.01
HIF-1a CAD	0.02 ± 0.01	0.03 ± 0.00	0.10 ± 0.01	0.06 ± 0.01	0.11 ± 0.01	0.68 ± 0.02	1.00 ± 0.01
6H-Notch-HIF linker	0.03 ± 0.01	0.07 ± 0.01	0.09 ± 0.01	0.07 ± 0.00	0.22 ± 0.01	0.52 ± 0.01	1.01 ± 0.01
Trx-6H-mNotch1 wt	0.11 ± 0.01	0.09 ± 0.00	0.16 ± 0.01	0.09 ± 0.01	0.18 ± 0.01	0.36 ± 0.01	0.99 ± 0.01
Trx-6H-mNotch1 S2*	0.12 ± 0.01	0.10 ± 0.01	0.14 ± 0.02	0.08 ± 0.00	0.17 ± 0.01	0.38 ± 0.01	1.00 ± 0.01
Trx-6H-mNotch1 S2* A-P	0.10 ± 0.01	0.09 ± 0.00	0.18 ± 0.01	0.09 ± 0.00	0.18 ± 0.01	0.35 ± 0.01	0.99 ± 0.01
Trx-6H-mNotch1 S2* I-Q	0.13 ± 0.02	0.11 ± 0.02	0.13 ± 0.03	0.07 ± 0.01	0.17 ± 0.00	0.38 ± 0.01	0.99 ± 0.01
Trx-6H-mNotch4 wt	0.11 ± 0.01	0.09 ± 0.00	0.17 ± 0.01	0.09 ± 0.01	0.18 ± 0.01	0.37 ± 0.00	1.00 ± 0.01
Trx-6H-mNotch4 P-A	0.10 ± 0.01	0.09 ± 0.00	0.16 ± 0.01	0.08 ± 0.01	0.18 ± 0.01	0.38 ± 0.02	0.99 ± 0.00
Trx-6H-mNotch4 Q-I	0.09 ± 0.01	0.08 ± 0.01	0.17 ± 0.01	0.09 ± 0.01	0.18 ± 0.01	0.38 ± 0.01	0.99 ± 0.00